

## Structure determination of proteins in $^2\text{H}_2\text{O}$ solution aided by a deuterium-decoupled 3D HCA(N)CO experiment

Kenji Ogura · Hiroyuki Kumeta · Fuyuhiko Inagaki

Received: 17 May 2010 / Accepted: 10 June 2010 / Published online: 24 June 2010  
© Springer Science+Business Media B.V. 2010

**Abstract** We developed an NMR pulse sequence, 3D HCA(N)CO, to correlate the chemical shifts of protein backbone  $^1\text{H}\alpha$  and  $^{13}\text{C}\alpha$  to those of  $^{13}\text{C}'$  in the preceding residue. By applying  $^2\text{H}$  decoupling, the experiment was accomplished with high sensitivity comparable to that of HCA(CO)N. When combined with HCACO, HCAN and HCA(CO)N, the HCA(N)CO sequence allows the sequential assignment using backbone  $^{13}\text{C}'$  and amide  $^{15}\text{N}$  chemical shifts without resort to backbone amide protons. This assignment strategy was demonstrated for  $^{13}\text{C}/^{15}\text{N}$ -labeled GB1 dissolved in  $^2\text{H}_2\text{O}$ . The quality of the GB1 structure determined in  $^2\text{H}_2\text{O}$  was similar to that determined in  $\text{H}_2\text{O}$  in spite of significantly smaller number of NOE correlations. Thus this strategy enables the determination of protein structures in  $^2\text{H}_2\text{O}$  or  $\text{H}_2\text{O}$  at high pH values.

**Keywords** HCA(N)CO ·  $^2\text{H}$  decoupling · GB1 · Structure determination

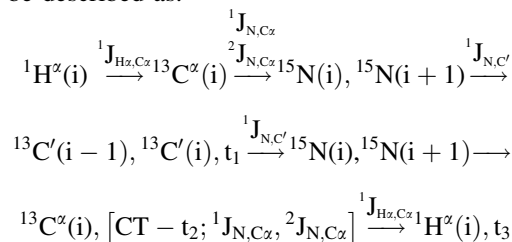
In protein NMR studies, backbone amide protons play an essential role in sequential resonance assignment of isotopically enriched proteins. Many NMR pulse sequences for  $^{13}\text{C}/^{15}\text{N}$ -labeled proteins have been designed to detect the correlations between amide protons and other nuclei (e.g.,  $^{15}\text{N}$ ,  $^{13}\text{C}'$ ,  $^{13}\text{C}\alpha$ , and  $^{13}\text{C}\beta$ ) via inter- and intra-residual J connectivity. HNCACB (or CBCANH) and CBCA(CO)NH experiments, in particular, are widely used

for sequential assignment as the chemical shifts of the  $^{13}\text{C}\alpha$  and  $^{13}\text{C}\beta$  carbons are characteristic of amino acid types and help position a sequentially connected stretch of amino acids within the primary sequence of the protein (Grzesiek and Bax 1992a, b; Wittekind and Müller 1993). Therefore, the correlations between  $^1\text{H}^{\text{N}}$  and  $^{13}\text{C}\alpha/^{13}\text{C}\beta$  are utilized as a common strategy for protein sequential backbone assignment. However, under alkaline conditions, this assignment strategy is not applicable since amide protons cannot be observed due to the rapid exchange of amide protons with the solvent protons. Therefore, protein NMR studies are restricted to solutions with pH of less than 7.5. To overcome this problem, Wang et al. (1995) proposed deuterium-decoupled 2D H(CA)N and H(CACO)N pulse sequences measured in  $^2\text{H}_2\text{O}$  solution to correlate  $\text{H}\alpha$  with the preceding and proceeding amide  $^{15}\text{N}$  nuclei, respectively. Furthermore, their alternative 3D version for the detection of the effects of the amide deuterium isotope on  $^{13}\text{C}\alpha$  chemical shifts has been described by Ottiger and Bax (1997). On the other hand, Kanelis et al. (2000) have proposed HACAN and (HB)CBCA(CO)N(CA)HA experiments to assign the proline-rich motif and polyproline-stretch, which has a lack of amide protons. However, as the sequential assignment strategy using these spectra is based on the chemical shift of amide  $^{15}\text{N}$  only, ambiguities in sequential assignment cannot be avoided. In this communication, a 3D experiment, HCA(N)CO, designed for  $^{13}\text{C}/^{15}\text{N}$ -labeled proteins dissolved in  $^2\text{H}_2\text{O}$ , is presented for the correlation of a pair of  $^1\text{H}\alpha$  and  $^{13}\text{C}\alpha$  chemical shifts to the  $^{13}\text{C}'$  chemical shift of the preceding residue. By combining HCA(N)CO with 3D HCAN, HCA(CO)N and HCACO, we propose a new sequential assignment strategy based on both the amide  $^{15}\text{N}$  and  $^{13}\text{C}'$  chemical shifts. This strategy enables the sequential resonance assignment of proteins without resort to amide protons and, therefore,

K. Ogura · H. Kumeta · F. Inagaki (✉)  
Department of Structural Biology, Faculty of Advanced Life  
Science, Hokkaido University, Kita 21 Nishi 11,  
Kita-ku, Sapporo 001-0021, Japan  
e-mail: finagaki@pharm.hokudai.ac.jp

enables the determination of protein structures in  $^2\text{H}_2\text{O}$  solution or at alkaline pH. We determined protein structures of GB1 in  $^2\text{H}_2\text{O}$  and in  $\text{H}_2\text{O}$ , and showed that structural determination in  $^2\text{H}_2\text{O}$  is practically applicable.

Figure 1 provides the pulse sequence of the deuterium-decoupled 3D HCA(N)CO experiment used to obtain inter-residue (and weaker intra-residue) connectivities between the  $^1\text{H}\alpha$ ,  $^{13}\text{C}\alpha$  and  $^{13}\text{C}'$  nuclei. The pulse sequence is a so-called ‘out-and-back’ style, and is similar to the gradient-enhanced 3D HCA(CO)N scheme described by Ottiger and Bax (1997). Briefly, the path of magnetization transfer can be described as:



The final magnetization transfer path from  $^{13}\text{C}\alpha$  to  $^1\text{H}\alpha$  uses a Rance–Kay style gradient-enhanced scheme (Palmer et al. 1991; Kay et al. 1992). For proteins dissolved in  $^2\text{H}_2\text{O}$ , the  $^{15}\text{N}$   $T_2$  elongation due to  $^2\text{H}$ -decoupling during

the  $^{15}\text{N}$  evolution or delay period is helpful to allow sensitivity enhancement of this experiment.

NMR experiments for the backbone resonance assignment were carried out at  $25^\circ\text{C}$  on a sample of  $^{13}\text{C}/^{15}\text{N}$ -labeled 1.2 mM *Streptococcal* GB1 domain dissolved in  $^2\text{H}_2\text{O}$ . The one- and three-dimensional spectra of HCACO (Kay et al. 1990; Grzesiek and Bax 1993; Zhang and Gmeiner 1996), HCA(CO)N, HCAN, and HCA(N)CO were recorded on a Varian Inova 600 spectrometer equipped with a  $^2\text{H}$  decoupling circuit, an HCN triple resonance probehead, and a  $z$ -axis pulsed field gradient amplifier/coil. To compare sensitivities between each experiment, all 1D spectra were measured with 16 scans. For 3D experiments, spectra were recorded as data matrices of  $56 \times 56 \times 600$  complex points, with acquisition times 25.6 ms of ( $t_1$ ,  $^{15}\text{N}$ ), 23.2 ms of ( $t_1$ ,  $^{13}\text{C}'$ ), 12.4 ms of ( $t_2$ ,  $^{13}\text{C}\alpha$ ), and 60 ms of ( $t_3$ ,  $^1\text{H}$ ). The number of scans for 3D experiments was 4, 8, 8, and 8, for HCACO, HCA(CO)N, HCAN, and HCA(N)CO, respectively. Other NMR experiments, for side chain resonance assignments and for obtaining distance restraints, were measured on a Varian Inova 500 spectrometer. The  $^{13}\text{C}$ -edited NOESY spectra were recorded using two samples dissolved in  $^2\text{H}_2\text{O}$  and  $\text{H}_2\text{O}$ . The  $^{15}\text{N}$ -edited NOESY spectrum was recorded using a sample

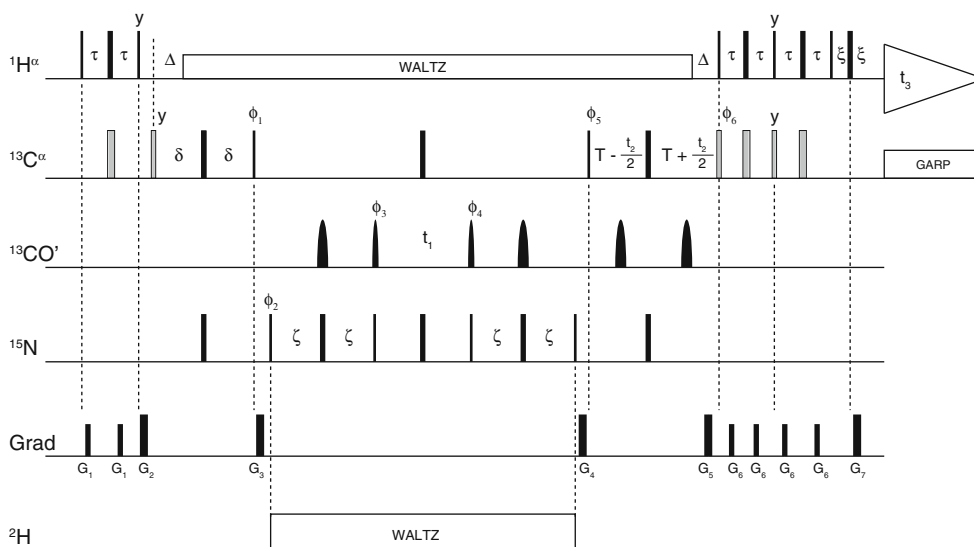


**Fig. 1** Pulse sequence of the deuterium-decoupled HCA(N)CO experiment. Narrow and wide pulses have flip angles of  $90^\circ$  and  $180^\circ$ , respectively. All pulses are applied along the  $x$ -axis, except where otherwise indicated.  $^1\text{H}$  broadband decoupling is performed with the 4.8 kHz WALTZ16 sequence.  $^2\text{H}$  decoupling is performed with the WALTZ16 sequence using 0.3 kHz rf field centered at 7.5 ppm.  $^{13}\text{C}\alpha$  decoupling during acquisition period is achieved using a 4.3 kHz GARP1 field. The carriers for the  $^{13}\text{C}\alpha$  and  $^{13}\text{C}'$  pulses are positioned at 56 and 174 ppm, respectively. The  $^{13}\text{C}\alpha$ -selective  $90^\circ$  and  $180^\circ$  pulses (black bars) are applied at rf field strengths of 4.6 and 10.3 kHz, respectively, which are adjusted so that they do not excite  $^{13}\text{C}'$  nuclei. The other  $^{13}\text{C}$  pulses on 56 ppm (grey bars) are applied

with an rf field of 15.6 kHz. Carbonyl pulses have a shaped amplitude profile corresponding to the center lobe of a  $\sin x/x$  function, and a duration of 89.2 and 80.8  $\mu\text{s}$  for the  $90^\circ$  and  $180^\circ$  pulses, respectively. Durations are  $\tau = 1.6$  ms,  $\Delta = 3.3$  ms,  $\delta = 14$  ms,  $\zeta = 14$  ms,  $T = 14$  ms, and  $\xi = 0.6$  ms. Phase cycling is as follows:  $\phi_1 = 4(y), 4(-y)$ ;  $\phi_2 = 8(x), 8(-x)$ ;  $\phi_3 = 2(x), 2(-x)$ ;  $\phi_4 = 60^\circ$ ;  $\phi_5 = x, -x$ ;  $\phi_6 = x$ ; Acq. =  $x, -x, -x, x, 2(-x, x, x, -x), x, -x, -x, x$ . Quadrature detection in  $t_2$  is obtained by inverting the polarity of  $G_5$  together with  $\phi_6$ . The strengths and durations of gradients are:  $G_1 = (0.5$  ms, 2 G/cm),  $G_2 = (1$  ms, 15 G/cm),  $G_3 = (0.3$  ms, 10 G/cm),  $G_4 = (0.4$  ms, 13 G/cm),  $G_5 = (2$  ms, 24 G/cm),  $G_6 = (0.5$  ms, 2 G/cm),  $G_7 = (0.5$  ms, 24 G/cm)

dissolved in H<sub>2</sub>O. For NOESY experiments, mixing time was set to 75 ms. Spectra were processed using the NMRPipe software package (Delaglio et al. 1995), and analyzed using the Sparky program (<http://www.cgl.ucsf.edu/home/sparky/>). The structures were calculated using the Cyana software package (Güntert 2004) based on the angular restraints from the Talos program (Cornilescu et al. 1999) and the inter-proton distance restraints from the NOESY spectra.

Figure 2 shows a comparison of the 1D spectra of HCACO, HCA(CO)N, HCAN, and HCA(N)CO with or without <sup>2</sup>H decoupling. As expected from the number of magnetization transfer paths and typical J coupling constant values of <sup>1</sup>J<sub>CαC'</sub> (~55 Hz), <sup>1</sup>J<sub>NCα</sub> (~11 Hz), and <sup>1</sup>J<sub>NC'</sub> (~15 Hz), HCACO (Fig. 2a) showed the highest sensitivity among the experiments. The sensitivities of other three spectra relative to the HCACO spectrum were 0.28 for HCA(CO)N (Fig. 2b), 0.47 for HCAN (Fig. 2c), and 0.13 for HCA(N)CO without <sup>2</sup>H decoupling (Fig. 2d). As the low sensitivity of the HCA(N)CO experiment was mainly due to the long delay time ( $4 \times \zeta \sim 56$  ms) for <sup>15</sup>N magnetization, we thought that <sup>2</sup>H decoupling during the <sup>15</sup>N evolution period or the delay would be effective in improving sensitivity. Figure 2e shows the HCA(N)CO spectrum with <sup>2</sup>H decoupling on the amide deuterium region. The sensitivity of the HCA(N)CO experiment by the introduction of <sup>2</sup>H decoupling was increased about two-fold, resulting in the relative sensitivities compared to those of the HCA(CO)N and HCACO to be 0.96 and 0.27, respectively. Therefore, we concluded that the HCA(N)CO experiment with <sup>2</sup>H decoupling can be practically applicable to the resonance assignment of <sup>13</sup>C/<sup>15</sup>N-labeled proteins dissolved in <sup>2</sup>H<sub>2</sub>O. Similar measurements were carried out at 4°C to increase a rotational correlation time in order to mimic the case for larger molecular weight proteins. Some weak and broad peaks were reduced in the HCA(CO)N and HCA(N)CO spectra. Further studies

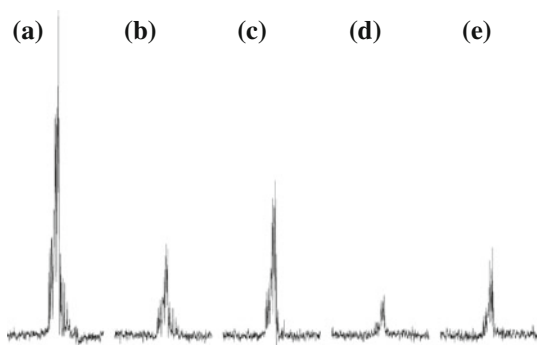


**Fig. 2** Comparison of 1D spectrum of 1.2 mM <sup>13</sup>C/<sup>15</sup>N-labeled GB1 in <sup>2</sup>H<sub>2</sub>O recorded at 600 MHz with 16 scans: **a** HCACO, **b** HCA(CO)N, **c** HCAN, **d** HCA(N)CO without <sup>2</sup>H decoupling, and **e** HCA(N)CO with <sup>2</sup>H decoupling

should be required for sensitivity of HCA(CO)N and HCA(N)CO in high molecular weight proteins.

Figure 3 shows strip plots taken from the HCACO (right strips) and HCA(N)CO (left strips) spectra of the GB1 domain in <sup>2</sup>H<sub>2</sub>O sliced at the <sup>13</sup>Cα and <sup>1</sup>Hα chemical shifts of the residues indicated along the *x*-axis. Solid lines connect the sequential assignment from Thr 17 to Ala 26 using the <sup>13</sup>C' chemical shifts. As described in the previous section, the HCA(N)CO experiment shows the correlation from the <sup>13</sup>Cα and <sup>1</sup>Hα to the stronger <sup>13</sup>C'(i - 1) and weaker <sup>13</sup>C'(i) signals. As the HCACO experiment shows the <sup>13</sup>C'(i) signals only, the <sup>13</sup>C'(i - 1) and <sup>13</sup>C'(i) signals can be easily distinguished on the HCA(N)CO strips. In Fig. 3, all the signals needed for the sequential assignment, except for <sup>13</sup>C'(i) signal of Ala 24, were detected on the HCA(N)CO and HCACO strips. This sequential assignment process using the <sup>13</sup>C' chemical shifts was confirmed by another approach using <sup>15</sup>N chemical shifts taken from both the HCAN and HCA(CO)N spectra (data not shown). Historically, the sequential backbone assignment strategy using <sup>15</sup>N and <sup>13</sup>C' chemical shifts was initially reported by Ikura et al. (1990). However, because the neighboring residues are connected by <sup>13</sup>C' chemical shifts derived from HNCO and HCACO spectra, this assignment strategy cannot be applied to samples dissolved in <sup>2</sup>H<sub>2</sub>O or under alkaline conditions. In such cases, the HCA(N)CO protocol can be used to obtain the <sup>13</sup>C' chemical shifts instead of the HNCO protocol.

To verify the usefulness of the present assignment strategy and to assess quality of the NMR structure that does not resort to backbone amide protons, we examined the precision of the protein structure determined in <sup>2</sup>H<sub>2</sub>O. For this purpose, the structures of the GB1 domain dissolved in <sup>2</sup>H<sub>2</sub>O and in H<sub>2</sub>O were calculated based on the angular restraints and inter-proton distance restraints using the Cyana software package. For the sample dissolved in <sup>2</sup>H<sub>2</sub>O, 749 cross peaks were incorporated from the <sup>13</sup>C-edited NOESY spectra whereas, for the sample dissolved in H<sub>2</sub>O, 488 and 806 cross peaks were incorporated from the <sup>15</sup>N-edited NOESY and <sup>13</sup>C-edited NOESY spectra, respectively. The structures of GB1 were calculated using NOE restraints obtained in the <sup>2</sup>H<sub>2</sub>O and H<sub>2</sub>O solutions (Fig. 4). The structural statistics are summarized in Table 1. Since the rmsd value of the main chain atoms (N, Cα and C') between both structures is 0.94 Å, and the rmsd value between the structure in <sup>2</sup>H<sub>2</sub>O and the atomic coordinates deposited as 3GB1 (Juszewski et al. 1999) is 0.95 Å, the structure calculated in <sup>2</sup>H<sub>2</sub>O is regarded as similar to that calculated in H<sub>2</sub>O. Surprisingly, despite a lack of distance restraints from the <sup>15</sup>N-edited NOESY spectrum, the structural rmsd value of backbone atoms in the <sup>2</sup>H<sub>2</sub>O solution (0.40 Å) is nearly equal to that in the H<sub>2</sub>O solution (0.48 Å). The structural rmsd value is

**Fig. 3** Strips from **a** 3D HCA(N)CO and **b** 3D HCACO spectra of GB1 in  $^2\text{H}_2\text{O}$  taken at the  $^{13}\text{C}\alpha$ ,  $^1\text{H}\alpha$  chemical shifts of the residue indicated along the  $x$ -axis. Solid and dashed lines indicate the sequential backbone assignment paths using  $^{13}\text{C}'$  chemical shifts from Thr 17 to Ala 26 of the GB1 domain

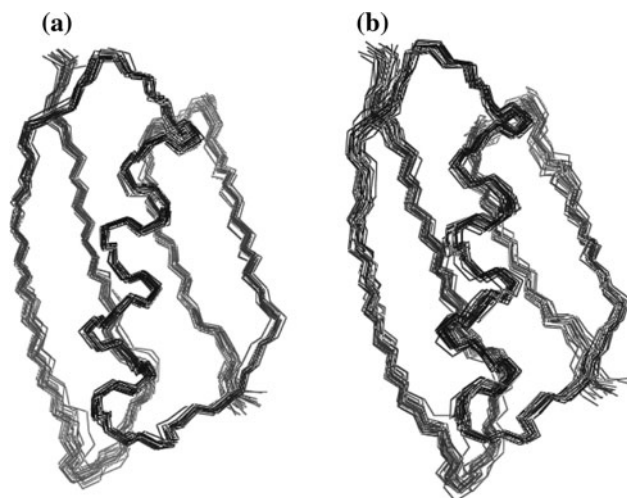
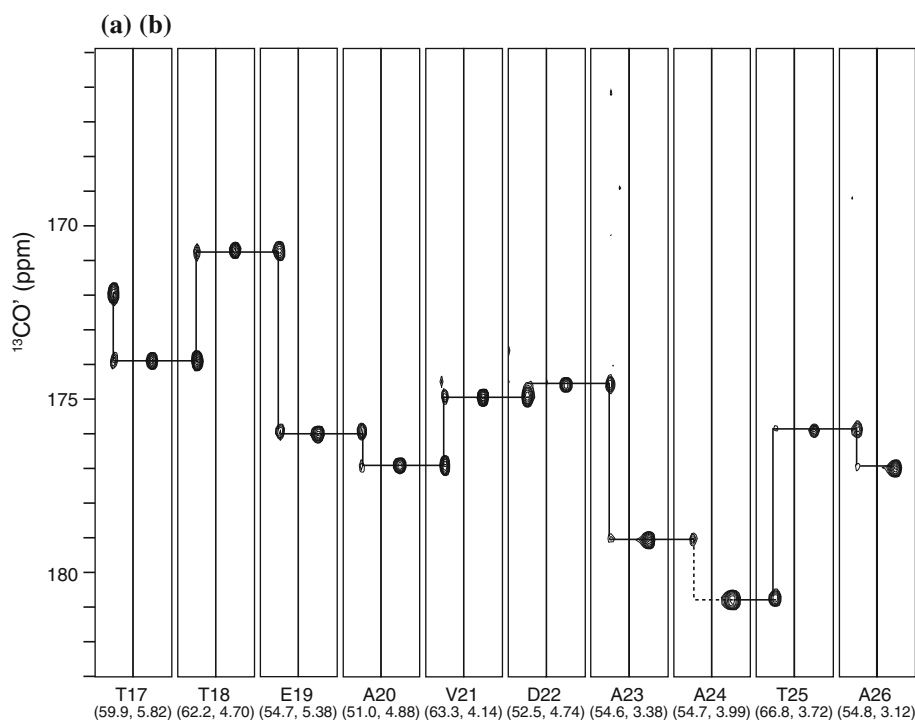


**Fig. 4** Superposition of the low energy 20 structures of the GB1 domain calculated using distance restraints derived from the  $^{13}\text{C}$ -edited NOESY in  $^2\text{H}_2\text{O}$  (**a**) and the  $^{13}\text{C}$ - and  $^{15}\text{N}$ -edited NOESY in  $\text{H}_2\text{O}$  (**b**)

generally considered to depend on the number of long-range ( $li - jl \geq 5$ ) distance restraints, while short-range ( $li - jl \leq 1$ ) distance restraints do not contribute to the improvement in structural rmsd values. As summarized in Table 1, in  $^2\text{H}_2\text{O}$  and  $\text{H}_2\text{O}$  solutions, 134 of 235 and 148 of 534 upper distance limits were categorized as long-range restraints, respectively. The structural rmsd values of GB1 in both solutions appears to be determined by the number of long-range distance restraints. However, the question arises as to why more long-range distance restraints are

**Table 1** NMR-derived restraints and structural statistics of the GB1 domain

	In $^2\text{H}_2\text{O}$	In $\text{H}_2\text{O}$
NOESY cross peaks		
$^{15}\text{N}$ -edited NOESY	–	488
$^{13}\text{C}$ -edited NOESY (aliphatic region)	636	722
$^{13}\text{C}$ -edited NOESY (aromatic region)	113	84
NOE upper distance restraints		
Short-range ( $li - jl \leq 1$ )	74	318
Medium-range ( $1 < li - jl < 5$ )	27	68
Long-range ( $li - jl \geq 5$ )	134	148
Dihedral angle restraints ( $\phi$ and $\psi$ )		
	108	108
Restraints violations		
Distance restraints violated by $>0.3 \text{ \AA}$	0	0
Torsion angle restraints violated by $>3^\circ$	0	0
Structural coordinates rmsd (3–55) ( $\text{\AA}$ )		
Backbone atoms	0.40	0.48
All heavy atoms	0.99	1.00

incorporated in the  $^2\text{H}_2\text{O}$  than in the  $\text{H}_2\text{O}$  solution. In the  $\text{H}_2\text{O}$  solution, aromatic and aliphatic protons are surrounded by exchangeable proton spins; i.e., amide protons and water molecules bound to the protein surface. Since cross- and transverse-relaxation rates are affected by proton density around the individual protons, dilute proton spins allow the detection of long-distance dipolar interactions. In the  $^2\text{H}_2\text{O}$  solution, proton densities were comparably lower than those in the  $\text{H}_2\text{O}$  solution; therefore, the

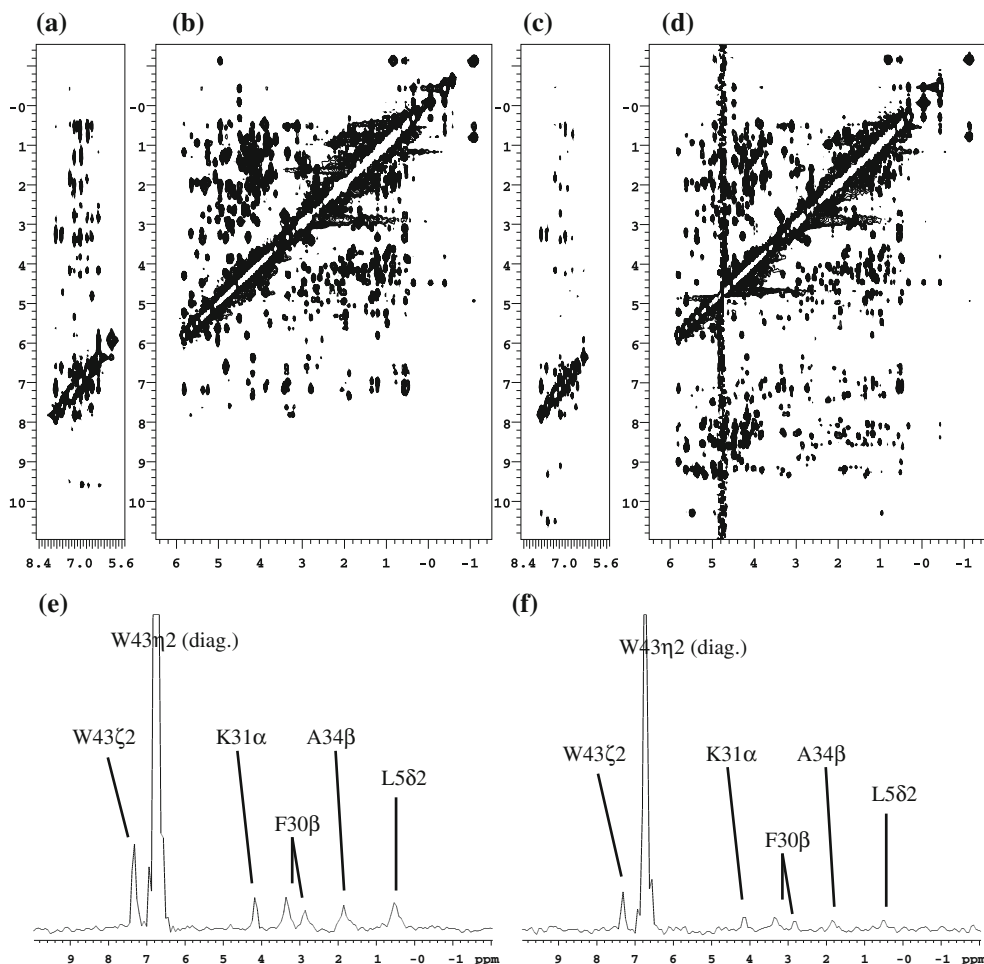


**Fig. 5** Skyline-projected spectra for  $F_1$ – $F_3$  planes taken from the 3D  $^{13}\text{C}$ -edited NOESY spectra of GB1 measured in  $^2\text{H}_2\text{O}$  (a, b) and  $\text{H}_2\text{O}$  (c, d), respectively. 3D spectra for aromatic (a, c) and aliphatic (b, d) regions were measured separately. All acquisition parameters were set to be equal in both measurements. No post-acquisition data

manipulation for solvent subtraction was applied. Vertical scaling of contour lines is identical for both sets of conditions. Slice traces for  $F_1$  axis at 6.75 ppm ( $F_3$ ) and 123.2 ppm ( $F_2$ ) corresponding to Trp43 $\eta$ 2 taken from the NOESY spectra measured in  $^2\text{H}_2\text{O}$  (e) and  $\text{H}_2\text{O}$  (f). Cross and diagonal peaks are shown with the resonance assignments

intensities and number of long-range cross peaks in the NOESY spectra are larger than those in  $\text{H}_2\text{O}$ . This additional long-range NOE information can be used to provide additional distance restraints in the structure refinement process. Figure 5 shows a spectral comparison of skyline-projected (a–d) and slice-traced (e and f)  $^{13}\text{C}$ -edited NOESY spectra measured in  $^2\text{H}_2\text{O}$  and  $\text{H}_2\text{O}$  solutions. Note that the cross peak intensities in  $^2\text{H}_2\text{O}$  are overall much higher than those in  $\text{H}_2\text{O}$ , though identical acquisition parameters were used for both solvents. In the aromatic region, in particular, the number and intensity of cross peaks were much larger in  $^2\text{H}_2\text{O}$  than those in  $\text{H}_2\text{O}$ . Actually, as shown in Table 1, a total of 113 and 84 cross peaks were detected from  $^{13}\text{C}$ -edited NOESY experiments for aromatic region in the  $^2\text{H}_2\text{O}$  and  $\text{H}_2\text{O}$  solutions, respectively. The additional cross peaks (ca. 30) in  $^2\text{H}_2\text{O}$  are thought to contribute to the improvement in structural rmsd. As a trial, omission of the cross peaks from the

aromatic region in  $^2\text{H}_2\text{O}$  resulted in a reduction in the structural rmsd from 0.40 Å to 0.62 Å. This result shows that distance restraints derived from aromatic protons are essential to improve the structural rmsd because aromatic groups play a key role in the construction of the hydrophobic core of the protein. Further theoretical considerations are required to clarify the relationship between proton density and NOESY cross peaks.

Additionally,  $^{13}\text{C}$ -edited NOESY experiments in  $^2\text{H}_2\text{O}$  solutions provide some practical advantages over those in  $\text{H}_2\text{O}$  solutions as follow; (1) residual  $\text{H}_2\text{O}$  signals does not interfere with NOESY cross peaks in the  $\text{C}\alpha$ – $\text{H}\alpha$  region, (2) increases in receiver gain allow the detection of relatively weak NOESY cross peaks, and (3) avoidance of baseline distortion and artifact noise generated from incomplete  $\text{H}_2\text{O}$  signal suppression allows the threshold level for peak picking to be lowered. Thus, it is concluded that the structure determination of small proteins dissolved

in  $^2\text{H}_2\text{O}$  is practically applicable, in spite of the lack of distance restraints derived from  $^{15}\text{N}$ -edited NOESY spectra. The present strategy also allows the determination of the structure of proteins at alkaline pH values. This can benefit structure determination by NMR since proteins are much more soluble at higher pH values.

In summary, we propose the HCA(N)CO pulse sequence that is useful for the sequential assignment of  $^{13}\text{C}/^{15}\text{N}$ -labeled proteins based on the  $^{13}\text{C}'$  chemical shifts. Deuterium decoupling allows to increase sensitivity comparable to that observed in HCA(CO)N experiment. The combination of the HCA(N)CO, HCACO, HCA(CO)N, and HCAN experiments is helpful for the sequential backbone assignment of proteins in  $^2\text{H}_2\text{O}$  and under alkaline conditions where assignment strategies based on amide protons is unsuccessful. Intriguingly, structure determination using distance restraints obtained in  $^2\text{H}_2\text{O}$  solutions shows similar or better results than determination using distance restraints obtained in  $\text{H}_2\text{O}$  solution in spite of a significantly smaller number of distance restraints. The present strategy establishes the sequential assignment and structure determination of small proteins dissolved in  $^2\text{H}_2\text{O}$ . Further quantitative analysis will be undertaken to investigate the difference in long-range distance restraints derived from  $^{13}\text{C}$ -edited NOESY spectra in  $\text{H}_2\text{O}$  and  $^2\text{H}_2\text{O}$  solutions. Furthermore, to evaluate the molecular weight limitation, we will apply this strategy to larger proteins.

**Acknowledgments** During the submission process of this manuscript, a similar pulse sequence, iH(CA)NCO, from Prof. Perttu Permi's group was published on-line in this journal. We thank Dr. Hong-Yu Hu, Shanghai Institute of Biochemistry, Academia Sinica, China, for providing the expression vector of the *Streptococcal* GB1 domain.

## References

- Cornilescu G, Delaglio F, Bax A (1999) Protein backbone angle restraints from searching a database for chemical shift and sequence homology. *J Biomol NMR* 13:289–302

- Delaglio F, Grzesiek S, Vuister GW, Zhu G, Pfeifer J, Bax A (1995) NMRPipe: a multidimensional spectral processing system based on UNIX pipes. *J Biomol NMR* 6:277–293
- Grzesiek S, Bax A (1992a) An efficient experiment for sequential backbone assignment of medium-sized isotopically enriched proteins. *J Magn Reson* 99:201–207
- Grzesiek S, Bax A (1992b) Correlating backbone amide and side-chain resonances in larger proteins by multiple relayed triple resonance NMR. *J Am Chem Soc* 114:6291–6293
- Grzesiek S, Bax A (1993) The origin and removal of artifacts in 3D HCACO spectra of proteins uniformly enriched with C-13. *J Magn Reson Ser B* 102:103–106
- Güntert P (2004) Automated NMR structure calculation with CYANA. *Methods Mol Biol* 278:353–378
- Ikura M, Kay LE, Bax A (1990) A novel approach for sequential assignment of  $^1\text{H}$ ,  $^{13}\text{C}$ , and  $^{15}\text{N}$  spectra of proteins: heteronuclear triple-resonance three-dimensional NMR spectroscopy. Application to calmodulin. *Biochemistry* 29:4659–4667
- Juszewski K, Gronenborn AM, Clore M (1999) Improving the packing and accuracy of NMR structures with a pseudopotential for the radius of gyration. *J Am Chem Soc* 121:2337–2338
- Kanelis V, Donaldson L, Muhandiram DR, Rotin D, Forman-Kay JD, Kay LE (2000) Sequential assignment of proline-rich regions in proteins: application to modular binding domain complexes. *J Biomol NMR* 16:253–259
- Kay LE, Ikura M, Tschudin R, Bax A (1990) Three-dimensional triple-resonance NMR spectroscopy of isotopically enriched proteins. *J Magn Reson* 89:496–514
- Kay LE, Keifer P, Saarinen T (1992) Pure absorption gradient enhanced heteronuclear single quantum correlation spectroscopy with improved sensitivity. *J Am Chem Soc* 114:10663–10665
- Ottiger M, Bax A (1997) An empirical correlation between amide deuterium isotope effects on  $^{13}\text{C}\alpha$  chemical shifts and protein backbone conformation. *J Am Chem Soc* 119:8070–8075
- Palmer AG, Cavanagh J, Wright PE, Rance M (1991) Sensitivity improvement in proton-detected two-dimensional heteronuclear correlation NMR spectroscopy. *J Magn Reson* 93:151–170
- Wang AC, Grzesiek S, Tschudin R, Lodi PJ, Bax A (1995) Sequential backbone assignment of isotopically enriched proteins in  $\text{D}_2\text{O}$  by deuterium-decoupled HA(CA)N and HA(CACO)N. *J Biomol NMR* 5:376–382
- Wittekind M, Müller L (1993) HNCACB, a high-sensitivity 3D NMR experiment to correlate amide-proton and nitrogen resonances with alpha- and beta-carbon resonances in proteins. *J Magn Reson Ser B* 101:201–205
- Zhang W, Gmeiner WH (1996) Improved 3D gd-HCACO and gd-(H)CACO-TOCSY experiments for isotopically enriched proteins dissolved in  $\text{H}_2\text{O}$ . *J Biomol NMR* 7:247–250